DNA AND CELL BIOLOGY
Volume 29, Number 9, 2010

Pp. 487–498
DOI: 10.1089/dna.2009.0989

A Novel Predicted Bromodomain-Related Protein Affects Coordination Between Meiosis and Spermiogenesis in *Drosophila* and Is Required for Male Meiotic Cytokinesis

Laura M. Bergner,* F. Edward Hickman,* Kathleen H. Wood,* Carolyn M. Wakeman, Hunter H. Stone, Tessa J. Campbell, Samantha B. Lightcap, Sheena M. Favors, Amanda C. Aldridge, and Karen G. Hales

Temporal coordination of meiosis with spermatid morphogenesis is crucial for successful generation of mature sperm cells. We identified a recessive male sterile *Drosophila melanogaster* mutant, *mitoshell*, in which events of spermatid morphogenesis are initiated too early, before meiotic onset. Premature mitochondrial aggregation and fusion lead to an aberrant mitochondrial shell around premeiotic nuclei. Despite successful meiotic karyokinesis, improper mitochondrial localization in *mitoshell* testes is associated with defective astral central spindles and a lack of contractile rings, leading to meiotic cytokinesis failure. We mapped and cloned the *mitoshell* gene and found that it encodes a novel protein with a bromodomain-related region. It is conserved in some insect lineages. Bromodomains typically bind to histone acetyl-lysine residues and therefore are often associated with chromatin. The Mitoshell bromodomain-related region is predicted to have an alpha helical structure similar to that of bromodomains, but not all the crucial residues in the ligand-binding loops are conserved. We speculate that Mitoshell may participate in transcriptional regulation of spermatogenesis-specific genes, though perhaps with different ligand specificity compared to traditional bromodomains.

Introduction

Spermatogenesis in insects and mammals begins with germ line stem cell divisions that produce spermatogonia, which divide mitotically to generate spermatocytes. These cells undergo meiosis, and the resulting haploid spermatids then execute dramatic morphogenetic changes to generate mature sperm. This process is a suitable context for molecular dissection of cell biological phenomena, such as cytokinesis and mitochondrial morphogenesis, as well as events of developmental control and coordination. Spermatogenesis in *Drosophila melanogaster* involves precise coordination between two semi-independent pathways, meiosis and spermiogenesis, the latter involving the morphogenetic changes of various organelles as early spermatids become mature sperm cells (reviewed in Fuller, 1993). In wild-type males, meiotic onset occurs only when spermatocytes have enlarged and accumulated most transcripts needed after meiosis; additional regulatory mechanisms then ensure completion of meiosis before spermiogenesis occurs. Easily detectable hallmarks of spermiogenesis include aggregation of mitochondria in early haploid spermatids and subsequent fusion into the two giant mitochondrial derivatives that intertwine to form the spherical Nebenkern. The two derivatives within the Nebenkern then unfurl and elongate beside the growing flagellar axoneme (reviewed in Fuller, 1993).

Complex transcriptional and translational cascades coordinate meiosis with spermiogenesis (Fig. 1). The *always early* (*aly*) class of transcriptional regulators encode components of a chromatin-associated complex that activates genes required both for meiosis (*twine*, *boule*, and *cyclin B*) and for spermiogenesis (*cannonball* [*can*]-class genes) (reviewed in White-Cooper, 2010). Mutations in *aly*-class genes lead to a complete arrest at primary spermatocyte stages. Downstream genes often function within one pathway or the other but not both. The exceptions to this rule provide the needed crosstalk to delay spermiogenesis until meiosis is complete.

Within the meiosis pathway, Twine, the meiotic Cdc25 phosphatase, is a central mediator of meiotic onset but is not required for sperm tail growth; males homozygous for *twine* mutations make spermatids that have large 4n nuclei and that proceed through spermiogenesis (Alphey *et al.*, 1992; Courtot *et al.*, 1992; White-Cooper *et al.*, 1993; Sigrist *et al.*, 1995). Within the spermiogenesis pathway, the *can*-class genes, encoding testis-specific TATA binding protein–associated factors (TAFs), are crucial for the transcription of many genes required for sperm tail growth (Hiller *et al.*, 2004). Testis TAFs help to coordinate meiosis with spermiogenesis through

Department of Biology, Davidson College, Davidson, North Carolina.
*These three authors contributed equally to this work.

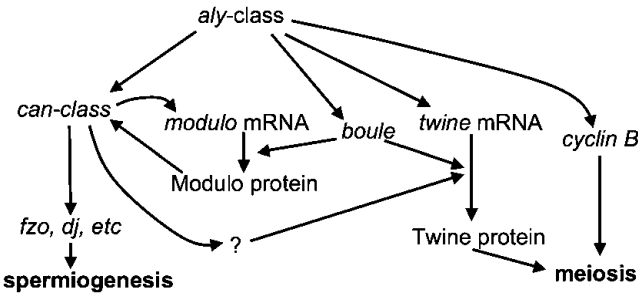

FIG. 1. Regulatory pathways coordinating meiosis and spermiogenesis in *Drosophila melanogaster*. The *always early* (*aly*)–class genes (including *comr*, *tomb*, *topi*, and *achi-vis*) control transcription of cell cycle regulators *twine* and *cyclin B* as well as spermiogenesis regulators from the *can* class of genes (including *mia*, *sa*, *nht*, and *mip40*) (reviewed in White-Cooper, 2010). The *can*-class gene products activate transcription of genes such as *fzo* and *dj* that is essential for the morphological changes of spermatid development. Crosstalk between the meiosis and spermiogenesis pathways includes the activity of *boule*, *modulo*, and an unidentified downstream target of *can*-class genes that facilitates *twine* translation (Maines and Wasserman, 1999; Mikhaylova *et al.*, 2006; White-Cooper, 2010).

transcriptional activation of an yet-unidentified mediator of translation of *twine* RNA (reviewed in White-Cooper, 2010). Translation of Twine also requires Boule, an RNA-binding protein whose expression is under the control of *aly*-class but not *can*-class genes (Maines and Wasserman, 1999). Twine, Boule, and other cell cycle regulators like Cyclin A and Roughex depend upon the testis-specific translation elongation factor eIF4G for proper timing of expression, as do unidentified spermiogenesis mediators; in *eIF4G* mutants, meiosis fails entirely, and only an initial aggregation of mitochondria forms beside the undivided nucleus before spermiogenesis arrest (Baker and Fuller, 2007; Franklin-Dumont *et al.*, 2007). Fine-tuning of the coordination between meiotic onset and sperm tail growth involves Modulo, a nucleolin homolog that, through a feedback loop, amplifies expression of *can*-class genes and that is itself dependent upon the meiotic activator Boule to be translated (Mikhaylova *et al.*, 2006).

Here we add to the roster of gene products that coordinate developmental pathways in the *Drosophila* testis. We characterize the recessive male sterile *D. melanogaster* mutant *mitoshell* that shows faulty coordination of meiosis and spermiogenesis, with mitochondria aggregating and fusing before completion of meiosis. We identify the associated gene and show that a protein containing a bromodomain-related region is required for proper developmental control of these events. We also explore mechanisms underlying meiotic cytokinesis failure in this mutant strain.

Materials and Methods

Fly husbandry, stocks, and fertility tests

Stocks and crosses were maintained at 25°C on an instant *Drosophila* medium from Ward's Natural Science. Fertility tests were performed by allowing test males to mate freely with three to five virgin females for 10 days, and the presence or absence of larvae was scored. Oregon R was the wild-type strain. The $mtsh^{Z2\text{-}2620}/CyO$, $mtsh^{Z2\text{-}3484}/CyO$, and $fzo^{Z3\text{-}4436}/TM6$ stocks were from the Zuker collection, as was the Z2-2588 line used as the background chromosome for the *mtsh* Zuker alleles (Koundakjian *et al.*, 2004). We obtained *P{RS3}CB-5520-3* (Ryder *et al.*, 2004) from the Szeged Drosophila Stock Center. The *GFP-anillin* stock (Goldbach *et al.*, 2010) was a gift from Philip Goldbach and Julie Brill (Hospital for Sick Children, Toronto, ON). The β *tubulin-EGFP* stock was created by Hiroki Oda and Yasuko Akiyama-Oda (JT Biohistory Research Hall). The *Sep2-GFP* (Silverman-Gavrila *et al.*, 2008) and $fzo^2/TM3$ (Hales and Fuller, 1997) stocks are as described. The following kit and stocks were from the Bloomington Drosophila Stock Center, each listed with FlyBase identifier:

Chromosome 2 Deficiency Kit (2002 version, including 81 stocks)
In(1)w^{m4h}, y^1; *Df(2L)TE29Aa-11, dp/CyO* (FBst0000179)
w^{1118}; *Df(2L)BSC111/CyO* (FBst0008836)
w^{1118}; *Df(2L)Exel7034/CyO* (FBst0007807)
w^{1118}; *Df(2L)ED611, P{3′.RS5 + 3.3′}ED611/SM6a* (FBst0009298)
y^1 *w*; *CyO, H{PΔ2-3}HoP2.1/*Bc^1 (FBst0002078)
w; $Kr^{If\text{-}1}/CyO$; $D^1/TM6C$, Sb^1 Tb^1 (FBst0007199)
w; noc^{Sco}/CyO, *S* bw^1 (FBst0003198)
A *w*; *Kr/CyO* stock was derived from *w*; $Kr^{If\text{-}1}/CyO$; $D^1/TM6C$, Sb^1 Tb^1 and *w*; noc^{Sco}/CyO, *S* bw^1 using appropriate crosses.

Imprecise P element excision

Flies homozygous for the *P{RS3}CB-5520-3* insertion were crossed to *y w*; *CyO, H{PΔ2-3}HoP2.1/*Bc^1. Resulting *w*; *P{RS3}CB-5520-3/CyO, H{PΔ2-3}HoP2.1* flies were crossed to *w*; *Kr/CyO*, and male offspring carrying potential excision chromosomes over *Kr* were identified by loss of *P{RS3}CB-5520-3*-associated eye color. These males were crossed individually to *w*; *Df(2L)BSC111/CyO* females. When viable, the *w*; *P{RS3}CB-5520-3 putative excision/Df(2L)BSC111* males were subjected to fertility tests. If sterility was detected, sibling *w*; *P{RS3}CB-5520-3 putative excision/CyO* males and females were crossed to create a balanced stock.

Generation of mtsh *flies marked with GFP-tagged transgenes*

Flies of genotype $mtsh^{Z2\text{-}2620}/CyO$ were crossed to *w*; *Kr/CyO*; *D/TM6C, Sb.* The *w*; $mtsh^{Z2\text{-}2620}/CyO$; *D/+* offspring were crossed to w/w^+; $mtsh^{Z2\text{-}2620}/CyO$; *TM6C, Sb/+* from which flies were selected to generate a *w*; $mtsh^{Z2\text{-}2620}/CyO$; *D/TM6C, Sb* stock. Simultaneously, *w*; β *tubulin-EGFP* flies (insert on the 3rd) were crossed to *w*; *Kr/CyO*; *D/TM6C, Sb.* The *w*; *Kr/+*; β *tubulin-EGFP/TM6C, Sb* and *w*; β *tubulin-EGFP/TM6C, Sb* offspring were crossed, from which *w*; *Kr/CyO*; β *tubulin-EGFP/TM6C, Sb* flies were used to make a stock. Then, *w*; $mtsh^{Z2\text{-}2620}/CyO$; *D/TM6C, Sb* flies were crossed to *w*; *Kr/CyO*; β *tubulin-EGFP/TM6C, Sb*, and *w*; $mtsh^{Z2\text{-}2620}/CyO$; β *tubulin-EGFP/TM6C, Sb* flies were used to make a stock. From that stock, *w*; $mtsh^{Z2\text{-}2620}/mtsh^{Z2\text{-}2620}$; β *tubulin-EGFP/TM6C, Sb* males (and their heterozygous siblings as controls) were subjected to testis dissection and fluorescence microscopy. The *Sep2-GFP* and *GFP-anillin* stocks were subjected to analogous crosses as described

for β *tubulin-EGFP* to generate *w*; $mtsh^{Z2\text{-}2620}$/*CyO*; *Sep2-GFP/TM6C* and *w*; $mtsh^{Z2\text{-}2620}$/*CyO*; *GFP-anillin/TM6C* stocks from which $mtsh^{Z2\text{-}2620}$ homozygotes carrying each transgene could be identified. These stocks were also crossed to $mtsh^{Z2\text{-}3484}$/*CyO* and $mtsh^{55207\text{-}12}$/*CyO* to create *mtsh* transheterozygotes carrying the *GFP-anillin* or β *tubulin-EGFP* transgenes.

Generation of mtsh; fzo *double mutants*

Males carrying the fzo^{2} (Hales and Fuller, 1997) and $fzo^{Z3\text{-}4436}$ (Koundakjian *et al.*, 2004) alleles balanced over *CyO* were crossed to *w*; *Kr/CyO*; *D/TM6C*, *Sb* virgins. Male *w*; *Kr/+*; *fzo/TM6C* offspring were crossed to w^{+}/*w*; *CyO/+*; *fzo/TM6C* females, and *w*; *Kr/CyO*; *fzo/TM6C* progeny were collected to create a stock for each *fzo* allele. These flies were then crossed to *w*; $mtsh^{Z2\text{-}2620}$/*CyO*; *Sep2-GFP/TM6C*, *Sb* flies. The *w*; $mtsh^{Z2\text{-}2620}$/*CyO*; *fzo/TM6C* progeny were collected to create balanced stocks for each *fzo* allele. We crossed these two stocks to generate *w*; $mtsh^{Z2\text{-}2620}$/$mtsh^{Z2\text{-}2620}$; fzo^{2}/$fzo^{Z3\text{-}4436}$ males for testis dissection. Siblings of genotype *w*; $mtsh^{Z2\text{-}2620}$/$mtsh^{Z2\text{-}2620}$; *fzo/TM6C* and *w*; $mtsh^{Z2\text{-}2620}$/*CyO*; fzo^{2}/$fzo^{Z3\text{-}4436}$ were also dissected and examined.

Microscopy of live squashed testis preparations

We dissected testes in TB1 buffer (7 mM K_2HPO_4, 7 mM KH_2PO_4 [pH 6.7], 80 mM KCl, 16 mM NaCl, 5 mM $MgCl_2$, and 1% PEG-6000), sometimes including 4 μg/mL Hoechst DNA stain (Sigma Life Science), and opened testes with forceps to allow cells to form a monolayer after introduction of a cover slip. Samples were examined with phase-contrast optics and/or under fluorescence with a Nikon Eclipse E600W or Olympus B201 microscope. Images were captured with a Nikon Coolpix 4500 camera or Spot Camera.

Sequencing of alleles

Using standard methods we purified genomic DNA from flies homozygous for each *mtsh* allele, as well as from homozygotes of the nonallelic *Z2-2588* male sterile Zuker collection strain as the background chromosome for $mtsh^{Z2\text{-}2620}$ and $mtsh^{Z2\text{-}3484}$. We amplified *CG7795* in two parts using the following primer pairs purchased from Integrated DNA Technologies: 5′-ACACGGGCTACATCCCATTATCTC-3′ and 5′-TCATTCCCAGGTACTTCTGTGCCA-3′, and 5′-CG GATGGCGTGCTGCCAAATATAA-3′ and 5′-CATGCTATT GGCGCAGGACATTGA-3′. Additional sequencing primers included the following: 5′-TCTGCTCCCTAGGGTTTCAGAA CA-3′, 5′-TTTGGATCGCAATCGCATGGTCAC-3′, 5′-ACAGT CGAAACTGTCGCGGTATGA-3′, 5′-AGCCAAGACCAGAA AGGTAAGGCT-3′, 5′-CTGCGCCGCTTTCCAATGAACTAA-3′, 5′-CAACGCCATGTAGATGCCAATGGT-3′, 5′-TAATGGTC ATTTGGCTTGGCTGGC-3′, 5′-GGATCATCTTTACGGTGCGC TGTT-3′, 5′-TGTGAACGACATGCTTTCCAAGCC-3′, 5′-CTGC AGATAACAGCGCACCGTAA-3′, 5′-GATAATGTGGCGGCTT GGAAAGC-3′, 5′-CTCCCGTTCTTTGGTCGCAACATT-3′, and 5′-AATGTTGCGACCAAAGAACGGGAG-3′.

Retrogen Inc. performed the sequencing reactions. Sequence differences in $mtsh^{Z2\text{-}2620}$ and $mtsh^{Z2\text{-}3484}$ compared to the background chromosome in *Z2-2588* were confirmed with sequence reads on both strands, using template DNA amplified separately in two independent reactions.

Sequence analysis

Homology searches were with BLAST (Altschul *et al.*, 1990) at the National Center for Biotechnology Information and FlyBase (Tweedie *et al.*, 2009) Web sites. Multiple sequence alignment was performed with ClustalW (Larkin *et al.*, 2007). In sequence similarity calculations, the ClustalW conserved but not semi-conserved residues were counted. Protein secondary structure prediction used the PROF algorithm (Rost and Sander, 1993) at the PredictProtein Web site (Rost *et al.*, 2004). Protein localization prediction was with WoLF PSORT (Horton *et al.*, 2007) and LOCtree (Nair and Rost, 2005). Nuclear localization signal prediction was with predictNLS (Cokol *et al.*, 2000).

Results

Mitochondria aggregate and fuse aberrantly early in mitoshell *mutants*

During spermatogenesis in wild-type *Drosophila* males, mitochondria are diffuse in the cytoplasm of mature primary spermatocytes (Fig. 2A, B) and gather in the central region of the meiotic spindle (Fig. 2C), subsequently aggregating and fusing in early round spermatids (Fig. 2D) into two giant derivatives that interwrap to form the Nebenkern, a phase-dark body adjacent to the phase-light nucleus (Fig. 2D–F) (Fuller, 1993). The Nebenkern unfurls and disentangles in a process that requires mitochondrial fission (Aldridge *et al.*, 2007). Mitochondria then elongate beside the flagellar axoneme (Fig. 2G, H). We identified from the Zuker collection of ethyl methane sulfate (EMS)–induced recessive nonlethal mutants (Koundakjian *et al.*, 2004; Wakimoto *et al.*, 2004) two allelic male sterile strains, $mtsh^{Z2\text{-}2620}$ and $mtsh^{Z2\text{-}3484}$, that showed aberrant aggregation of mitochondria in spermatocyes and spermatids. Homozygous adults were fully viable, and homozygous females were fertile.

In homozygous or transheterozygous *mtsh* males, primary spermatocytes appeared normal (Fig. 2I). Mitochondria aggregated abnormally early, in late primary spermatocytes before meiotic divisions, and in a single shell surrounding each premeiotic spermatocyte nucleus (Fig. 2J–L) instead of a separate body beside each postmeiotic nucleus as in wild type. Mutant spermatocytes underwent karyokinesis, with the resulting four nuclei staying adjacent to each other within the single mitochondrial shell. Under pressure from a cover slip, postmeiotic nuclei were visibly excluded from the intact mitochondrial shell and detectable by phase-contrast microscopy and Hoescht staining (Fig. 2N, O). However, Hoescht staining of nuclei completely surrounded by an intact mitochondrial shell (in a preparation not fully squashed) was undetectable, with no nuclei seen elsewhere (not shown), apparently an artifactual result of mitochondria inhibiting entry of the stain or transmission of fluorescence. In cells at a slightly later stage, presumably after undergoing mitochondrial fission and dissociation, cover slip pressure forced the single mitochondrial aggregate into four lobes (Fig. 2P). Hoescht staining indicated that nuclei sometimes, but not always, remained associated these lobes when under cover slip pressure (not shown). Meiotic cytokinesis was never observed in *mtsh* testes. Spermatid bundle elongation and other subsequent events of spermiogenesis occurred in *mtsh* mutant flies (Fig. 2Q). Spermatid tails appeared

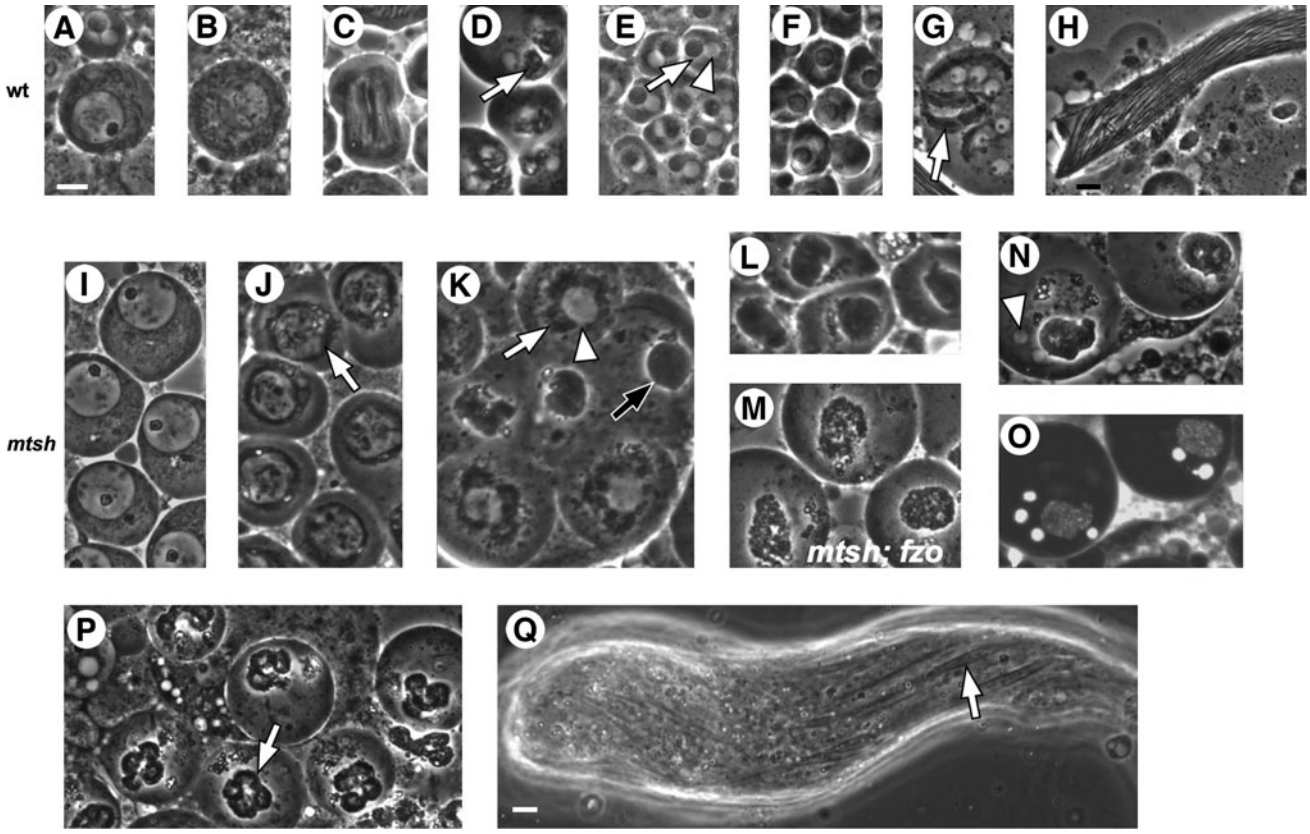

FIG. 2. In *mtsh* spermatogenesis, mitochondria aggregate and fuse prematurely, and meiotic cytokinesis fails. Phase-contrast (**A–N** and **P–Q**) and fluorescence (**O**) micrographs of live squashed preparations of testes from wild-type (**A–H**), $mtsh^{Z2\text{-}2620}/mtsh^{Z2\text{-}2620}$ (**I–L** and **N–Q**), and $mtsh^{Z2\text{-}2620}/mtsh^{Z2\text{-}2620}$; $fzo^{2}/fzo^{Z3\text{-}4436}$ (**M**) males. Wild-type primary spermatocyte (**A**) includes a large phase-light nucleus with phase-dark nucleolus; small, phase-dark mitochondria are diffuse in the cytoplasm. In spermatocytes approaching meiosis (**B**), the nucleolus becomes less distinct, and mitochondria remain diffuse. In wild-type meiosis I (**C**) phase-dark mitochondria are aligned on the spindle. (**D**) After meiosis, mitochondria aggregate (arrow) and fuse beside each daughter nucleus. In early round spermatids (**E, F**), mitochondrial derivatives form a spherical phase-dark Nebenkern (arrow) beside each phase-light nucleus (arrowhead); the size of the Nebenkern is not affected in preparations not fully squashed (**F**). Mitochondria unfurl and elongate (**G**, arrow) and later stretch the full length of each cell within a spermatid bundle (**H**, partial view). Spermatocytes from *mtsh* males appear normal (**I**) but show aberrant and premature mitochondrial aggregation (**J**, arrow) in cells approaching the first meiotic division. (**K**) Cyst of *mtsh* spermatocytes in which mitochondrial aggregation has progressed further in some cells than in others. Aggregating mitochondria (white arrow) appear to form a shell (black arrow) eclipsing each premeiotic nucleus (white arrowhead). (**L**) Live testis preparation not fully squashed; *mtsh* nuclei appear surrounded by mitochondrial shells. Compare to panel (**F**). (**N, O**) Fully squashed and Hoescht-stained *mtsh* postmeiotic cells under phase-contrast optics (**N**) and fluorescence (**O**); four smaller nuclei (e.g., arrowhead) of roughly the size found in normal haploid spermatids (see panel **E**) have escaped one mitochondrial shell. (**P**) Later-stage *mtsh* spermatids squashed after mitochondrial fission and unfurling; each mitochondrial aggregate separates into four nucleus-associated lobes (arrow) under cover slip pressure. (**Q**) Elongating spermatid bundles in *mtsh*, with wide parallel arrays of elongating mitochondria (arrow). Transheterozygotes showed identical phenotypes. Scale bars 10 μm. Panels (**A–G**) and (**I–P**) at same magnification; (**H**) and (**Q**) at same magnification.

irregularly packed (Fig. 2Q, arrow; compare to Fig. 2H), consistent with the presence of multinucleate spermatids, as in *fwd* mutant males (Brill *et al.*, 2000). The resulting sperm cells were not individualized, a common phenotype in male sterile strains with sperm structural defects (reviewed in Fuller, 1993). The $mtsh^{Z2\text{-}2620}$ and $mtsh^{Z2\text{-}3484}$ mutant phenotypes were fully penetrant.

To determine whether mitochondrial fusion accompanies premature mitochondrial aggregation in *mtsh* mutants, we generated flies homozygous for $mtsh^{Z2\text{-}2620}$ and transheterozygous for two alleles of *fzo.* Fzo is a testis-specific mediator of mitochondrial fusion that in wild type is detectable only during and after telophase of meiosis II (Hales and Fuller, 1997). The *mtsh*; *fzo* double mutants differed from *mtsh* flies, with the double mutants showing aggregated but fragmented mitochondria (Fig. 2M), compared to the smooth and cohesive mitochondrial shell in *mtsh*/*mtsh* testes (Fig. 2K, L). These results suggest that in flies homozygous for only *mtsh*, premature Fzo-mediated mitochondrial fusion accompanies premature mitochondrial aggregation.

mitoshell *corresponds to CG7795*

To map *mitoshell*, we crossed $mtsh^{Z2\text{-}2620}/CyO$ flies to the 81 strains that comprised the 2002 Chromosome 2 Deficiency

Kit from the Bloomington Drosophila Stock Center and tested the $mtsh^{Z2\text{-}2620}$/deficiency offspring for fertility. The $mtsh^{Z2\text{-}2620}$ allele failed to complement *Df(2L)TE29Aa-11*, which lacks polytene region 28E4; 29C1 (Tweedie *et al.*, 2009). *Df(2L)TE29Aa-11*/$mtsh^{Z2\text{-}2620}$ flies had an identically severe phenotype to the $mtsh^{Z2\text{-}2620}$ or $mtsh^{Z2\text{-}3484}$ homozygotes, suggesting that the EMS alleles from the Zuker collection were either null alleles or very strong hypomorphs. We obtained additional deficiencies in the region and found that *Df(2L)BSC111* (28F5; 29B1), also failed to complement $mtsh^{Z2\text{-}3484}$, while *Df(2L)Exel7034* (28E1; 28F1) and *Df(2L)ED611* (29B4; 29C3) complemented the mutation. *Df(2L)BSC111* lacks the molecularly defined interval 2L: 8,240,266-8,362,842 (FlyBase release 2010_02) (Tweedie *et al.*, 2009), encompassing ~23 genes. Four of these genes, *CG7795*, *CG8086*, *CG8292*, and *CG8349*, were recorded in the FlyAtlas database (Chintapalli *et al.*, 2007) as having markedly enriched expression only in the testis. We viewed these genes as strong candidates since mutant *mitoshell* flies are male sterile but fully viable and female fertile. We amplified and sequenced *CG7795* from $mtsh^{Z2\text{-}2620}$ and $mtsh^{Z2\text{-}3484}$ homozygotes as well as from homozygotes of a different, nonallelic Zuker collection second chromosome stock (*Z2-2588*) as the background chromosome. We found that $mtsh^{Z2\text{-}2620}$ and $mtsh^{Z2\text{-}3484}$ each contained a nonsense mutation at a different position in *CG7795* (Fig. 3A), while the *Z2-2588* background chromosome contained an open reading frame that matched the *CG7795* reference sequence in the genome database (Tweedie *et al.*, 2009). Sequence analysis of a different candidate gene, *CG8292*, revealed no differences between *mtsh* alleles and the background chromosome. We did not obtain sequence data for *CG8086* and *CG8349.*

To generate new alleles by imprecise P element excision (Voelker *et al.*, 1984) and to confirm that *CG7795* represented *mitoshell*, we mobilized the homozygous viable and fertile *P{RS3}CB-5520-3* insertion (Ryder *et al.*, 2004; Tweedie *et al.*, 2009), located just upstream (13 and 36 bp, respectively) from the two predicted *CG7795* transcriptional start sites (Fig. 3A), by crossing in the *PΔ2-3* transgene encoding transposase (Tweedie *et al.*, 2009). Of 79 independent lines showing loss of the *P{RS3}CB-5520-3*-associated eye color, 2 were recessive male sterile and failed to complement $mtsh^{Z2\text{-}2620}$ and $mtsh^{Z2\text{-}3484}$. Homozygotes for one of the P element excision alleles, $mtsh^{55207\text{-}12}$, showed the same severe phenotype as the Zuker collection alleles, while $mtsh^{55201\text{-}3}$ was hypomorphic, with some normal-sized Nebenkerns observed. To determine the molecular lesion in the severe P element excision allele $mtsh^{55207\text{-}12}$, we amplified and sequenced the region surrounding the former P element insertion site. We found that $mtsh^{55207\text{-}12}$ contained a 751 bp deletion, which removed the predicted *CG7795* transcription start site, the 5′ untranslated region, and 434 bp of the coding region (Fig. 3A). Twenty base pairs of the P element were left behind. The deletion left intact the region upstream from the P element insertion site toward the next closest gene *CG7787*, whose transcriptional start site is predicted to be about 400 bp away. We were unable to amplify the region surrounding the P element insertion site in the hypomorphic allele $mtsh^{55201\text{-}3}$ allele, suggesting that a significant portion of the P element may be retained/and or at least one primer-binding site may be deleted. The nature of the lesions in the three molecularly characterized *mitoshell* alleles together indicates that *CG7795* represents *mitoshell*.

mitoshell/CG7795 *encodes a novel protein with a bromodomain-related region, conserved in some insect lineages*

The *mitoshell/CG7795* gene is annotated to encompass bases 8,316,889–8,319,920 on the minus strand of *D. melanogaster* chromosome 2 (FlyBase release 2010_02) (Tweedie *et al.*, 2009). Two transcripts of five and six exons are predicted, respectively, encoding 649 and 604 amino acid polypeptides. The shorter predicted protein isoform lacks carboxy terminal residues due to retention of a 27 bp exon containing a stop codon. The single testis expressed sequence tag (EST) in GenBank (accession BE976148) corresponding to *CG7795* matches the transcript encoding the longer protein isoform, while a single EST from embryonic tissue (accession CK131376) matches the transcript encoding the trucated isoform. Mtsh is conserved only in Diptera, Lepidoptera, and Coleoptera; all predicted orthologs match the longer predicted *D. melanogaster* protein isoform. Among orthologs in the other 11 sequenced *Drosophila* species, amino acid identity/similarity to *D. melanogaster* Mtsh ranges from 89%/95% in *Drosophila simulans* to 42%/62% in *Drosophila grimshawi* (Fig. 3B). In the obscura subgroup of *Drosophila* species (but not in *D. melanogaster*), the Mtsh orthologs also include a domain common to DNA polymerase III subunits tau and gamma (Jarvis *et al.*, 2005); the tau and gamma subunits are necessary for oligomerization of the DnaX complex, which is required for assembling the two DNA polymerase III core complexes on the leading and lagging strands (Gao and McHenry, 2001; Glover *et al.*, 2001; McHenry, 2003). *D. melanogaster* Mtsh is 27% identical/46% similar and 24% identical/42% similar, respectively, to orthologs in the mosquitoes *Aedes egyptii* and *Culex quinquefasciatus*. An ortholog in the flour beetle *Tribolium castaneum* shares 14% identity and 27% similarity to Mtsh. The genomes of the mosquito *Anopheles gambiae* and the silkworm *Bombyx mori* include unannotated sequences predicted to encode Mtsh homologs; however, no homolog is detected in sequenced genomes from Hymenoptera or more distantly related insect orders.

Sequence alignments indicate two conserved domains, of 137 and 105 amino acids, respectively (Fig. 3B–D), that are both predicted to be highly alpha helical (PROF algorithm; PredictProtein) (Rost *et al.*, 2004). Region 1 contains no recognizable motifs. Region 2 in the *A. egyptii* and *C. quinquefasciatus* orthologs is annotated in the Conserved Domain Database (Marchler-Bauer *et al.*, 2009) to be similar to bromodomains, a motif with four alpha helices and two loops that typically confers chromatin association via binding to acetylated histones (reviewed in Loyola and Almouzni, 2004). The bromodomain-like region 2 shows identical predicted alpha helical profiles among the Mtsh orthologs despite some sequence divergence. The predicted alpha helical profile also matches that of known bromodomains except at the amino terminal region where Mtsh and orthologs have two shorter predicted helices in the region of the single longer bromodomain Z helix (Fig. 3E). Of the 11 highly conserved residues found in most bromodomains, Mtsh and orthologs include 5 exact matches plus 2 others that are very

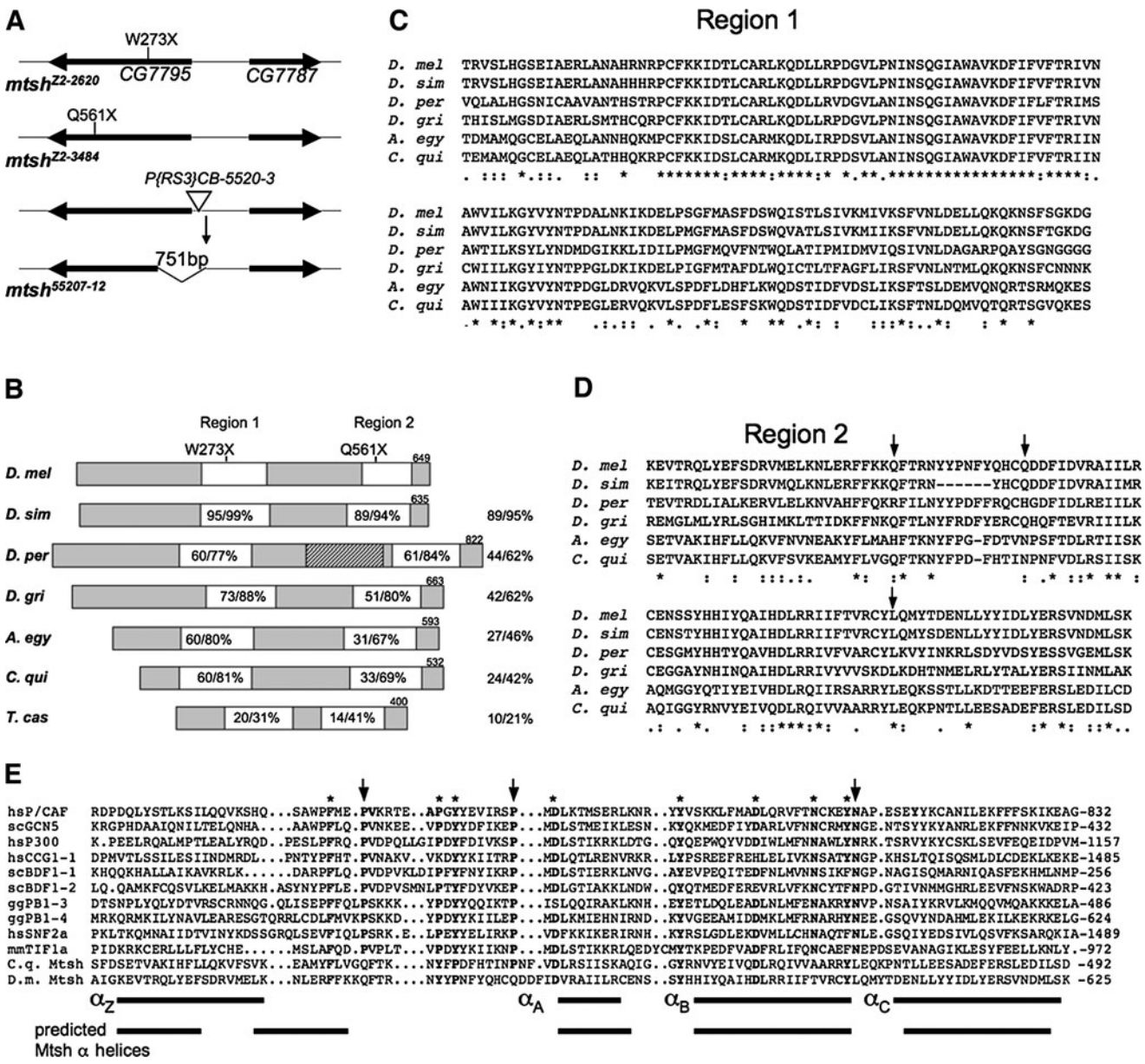

FIG. 3. The *mitoshell* gene corresponds to *CG7795* and encodes a protein containing a bromodomain-related region. (**A**) Schematic depiction of the *CG7795* region in polytene interval 29A on chromosome 2, showing the mutations in three *mtsh* alleles. The Zuker collection alleles $mtsh^{Z2\text{-}2620}$ and $mtsh^{Z2\text{-}3484}$ each have a unique nonsense mutation in *CG7795*. Mobilization of the *P{RS3}CB-5520-3* homozygous viable and fertile transposable element (triangle) led to the $mtsh^{55207\text{-}12}$ allele that lacks 751 bp, including the transcriptional and translational start sites of *CG7795*, but not affecting the adjacent gene *CG7787*. (**B**) Schematic diagram of Mtsh and its orthologs in 3 of the 11 other sequenced *Drosophila* species (*D. simulans* representing the closest neighbor, *D. persimilis* representing the obscura subgroup, and *D. grimshawi* representing the most distantly related), as well as *Aedes egyptii*, *Culex quinquefasciatus*, and *Tribolium castaneum*. Protein sizes are indicated at top right of each. The locations of nonsense mutations in $mtsh^{Z2\text{-}2620}$ and $mtsh^{Z2\text{-}3484}$ are indicated in regions 1 and 2 respectively. Amino acid identity/similarity to *D. melanogaster* Mtsh is shown at right for each full protein and within the white boxes for the highly conserved regions 1 and 2. The stippled box is a region found only in the obscura group of *Drosophila* species that resembles a domain of DNA polymerase III subunits tau and gamma. (**C**) and (**D**) ClustalW sequence lineups of the highly conserved regions 1 and 2 in Mtsh and Dipteran orthologs. Asterisks indicate identical residues, and double and single dots indicate the strongly and weakly similar residues, respectively. Arrows indicate sites corresponding to those most crucial for binding to acetylated lysine in typical bromodomains; also indicated with arrows in panel (**E**). (**E**) Sequence lineup comparing the bromodomain-related region (region 2) in Mtsh and the *C. quinquefasciatus* ortholog (bottom two rows) with 10 known bromodomains. Adapted from Dhalluin *et al.* (1999), with bromodomain-containing proteins as described therein. Arrows indicate the most highly conserved bromodomain residues. Asterisks indicate other highly conserved bromodomain residues. At bottom, the known four alpha helical regions of bromodomains are indicated, juxtaposed with the predicted alpha helical regions of Mtsh.

close in location and switched in position (Fig. 3E). However, none of the three residues that are absolutely conserved in bromodomains and important for binding to acetylated lysines (arrows in Fig. 3D, E) are conserved in Mtsh and orthologs (Mujtaba *et al.*, 2007). At the amino acid position between the B and C helices where a crucial bromodomain asparagine (rightmost arrow, Fig. 3E) forms a hydrogen bond with acetylated lysine (reviewed in Zeng and Zhou, 2002), Mtsh and orthologs contain an invariant leucine (lower arrow, Fig. 3D). Mtsh is predicted to be a soluble nuclear protein by WoLF PSORT (Horton *et al.*, 2007) and a nuclear DNA-binding protein by LOCtree (Nair and Rost, 2005), though no nuclear localization signal is detected by PredictNLS (Cokol *et al.*, 2000).

The mitoshell *cytokinesis failure results from a spindle defect and aberrant localization of contractile ring components*

To determine the basis of the meiotic cytokinesis failure in *mtsh* mutants, we crossed into $mtsh^{Z2\text{-}2620}$ flies transgenes encoding GFP- or EGFP-tagged versions of β tubulin, anillin, and Sep2, and examined the appropriate structures in *mtsh* homozygous and transheterozygous mutant testes under fluorescence microscopy. Cytokinesis depends in part upon formation and contraction of a contractile ring, whose cortical position is determined by signals from an equatorial region of overlapping antipolar spindle microtubules (reviewed in Barr and Gruneberg, 2007). We asked whether *mtsh* meiotic spindles in were intact by observing β tubulin-GFP localization in cells from dissected testes. In most primary spermatocytes whose mitochondria had aggregated but not yet fused, centrosomes were in the process of separating (not shown). Aberrant meiosis I spindles were detectable in the subset of cells with aggregated mitochondria just before mitochondrial fusion: *mtsh* cells in meiosis I lacked the overlapping astral microtubules in the central spindle region normally seen in wild type (Fig. 4A–D). The region corresponding to the anastral spindle described by Rebollo *et al.* (2004) was still intact in *mtsh*, and some non-overlapping astral microtubules were present. The most advanced meiotic spindle we observed, as determined by Hoescht costaining (not shown), was at metaphase I. Mitochondrial fusion at that time led to an artifact of the phenotype, namely that neither spindle fluorescence nor DNA fluorescence could be detected from within fully formed mitochondrial shells (with these structures visible nowhere else in the cell), so no further spindle assessment could be made after metaphase I. The fact that meiotic karyokinesis gave rise to four nuclei of roughly normal size (Fig. 2N–P) indicated that meiosis is not fully arrested and that parts of the spindle, such as perhaps the anastral spindle, are functioning normally within the mitochondrial shell through meiosis II.

In wild-type cells, the anillin protein cycles from the nucleus at interphase to the cell cortex during mitosis or meiosis; at the cortex, anillin gradually becomes more tightly localized to the cleavage furrow and contractile ring, where it helps orchestrate the recruitment of other ring proteins like septins, actin, and myosin (reviewed in Hickson and O'Farrell, 2008). The tight localization of anillin at the equatorial cortex in anaphase and telophase depends upon Pebble GEF-mediated Rho GTPase activation signals from the central spindle (reviewed in Hickson and O'Farrell, 2008). GFP-anillin has normal nuclear localization in *mtsh* primary spermatocytes (Fig. 5A–D) but is aberrantly localized in male meiotic cells, with only diffuse cortical localization instead of focusing into a tight ring (Fig. 5E–H). Sep2-GFP, another contractile ring component, localized in the ring in wild-type male meiotic cells but was not detected at the cell cortex in *mtsh* meiotic cells (not shown).

Discussion

The predicted bromodomain-related protein Mtsh is required for coordination of events in *Drosophila* spermatogenesis. We identified two alleles of *mtsh* from the Zuker collection of EMS-induced nonlethal mutants (Koundakjian *et al.*, 2004) and generated two additional P element excision alleles. The alleles have molecular lesions in *CG7795*, with the two EMS-induced alleles each containing a different nonsense mutation not seen in the background chromosome. The null P element excision allele $mtsh^{55207\text{-}12}$ is a small deletion of the 5′ portion of *CG7795*, including the transcriptional and translational start sites, and does not affect neighboring genes. The less severe phenotype of the P element excision allele $mtsh^{55201\text{-}34}$ may result from retention of a part of the P element and/or deletion of an upstream regulatory element, based on preliminary results. The *mtsh* gene appears to be required only in the testis, as homozygous individuals are completely viable, and homozygous null females are fully fertile. This observation is consistent with expression data in the FlyAtlas database (Chintapalli *et al.*, 2007), indicating that the testis is the only tissue in which *mtsh/CG7795* shows significantly enriched expression.

In the absence of functional Mtsh protein, mitochondrial aggregation (an early event of spermiogenesis) occurred at or before meiotic onset instead of at the end of meiosis. We demonstrated that mitochondria also fused prematurely, as the presence of nonfunctional testis mitofusin Fzo in double mutant *mtsh*; *fzo* flies resulted in fragmented mitochondrial shells compared to those seen in *mtsh* alone. In wild type, Fzo is first detectable at the end of telophase II (Hales and Fuller, 1997). In *mtsh*, mitochondria fused into a shell around the time of metaphase I, as the fully formed shell subsequently obscured observation of interior fluorescence from spindles or DNA at later stages. The abnormally early function of Fzo in *mtsh* indicated early Fzo expression and confirmed that multiple events of spermiogenesis occur prematurely.

Meiotic karyokinesis eventually occurred in *mtsh* homozygous males, but meiotic cytokinesis failed. The aberrant postmeiotic spermatids each with four haploid nuclei showed axoneme growth. Sperm individualization did not occur, as is typical when sperm morphology is defective (Fuller, 1993). This phenotype differs from other mutants known to affect meiosis/spermiogenesis coordination: in *aly*- and *can*-class mutant males, all aspects of sperm development are arrested at primary spermatocyte stages (reviewed in White-Cooper, 2010), and in *twine* mutants, meiosis fails but spermiogenesis proceeds, leading to a single 4n nucleus per cell associated with a large growing sperm tail (Alphey *et al.*, 1992; Courtot *et al.*, 1992; White-Cooper *et al.*, 1993; Sigrist *et al.*, 1995). In males mutant for *eIF4G*, meiosis is arrested, and only an initial mitochondrial cloud forms before spermiogenesis arrests as well (Baker and Fuller, 2007;

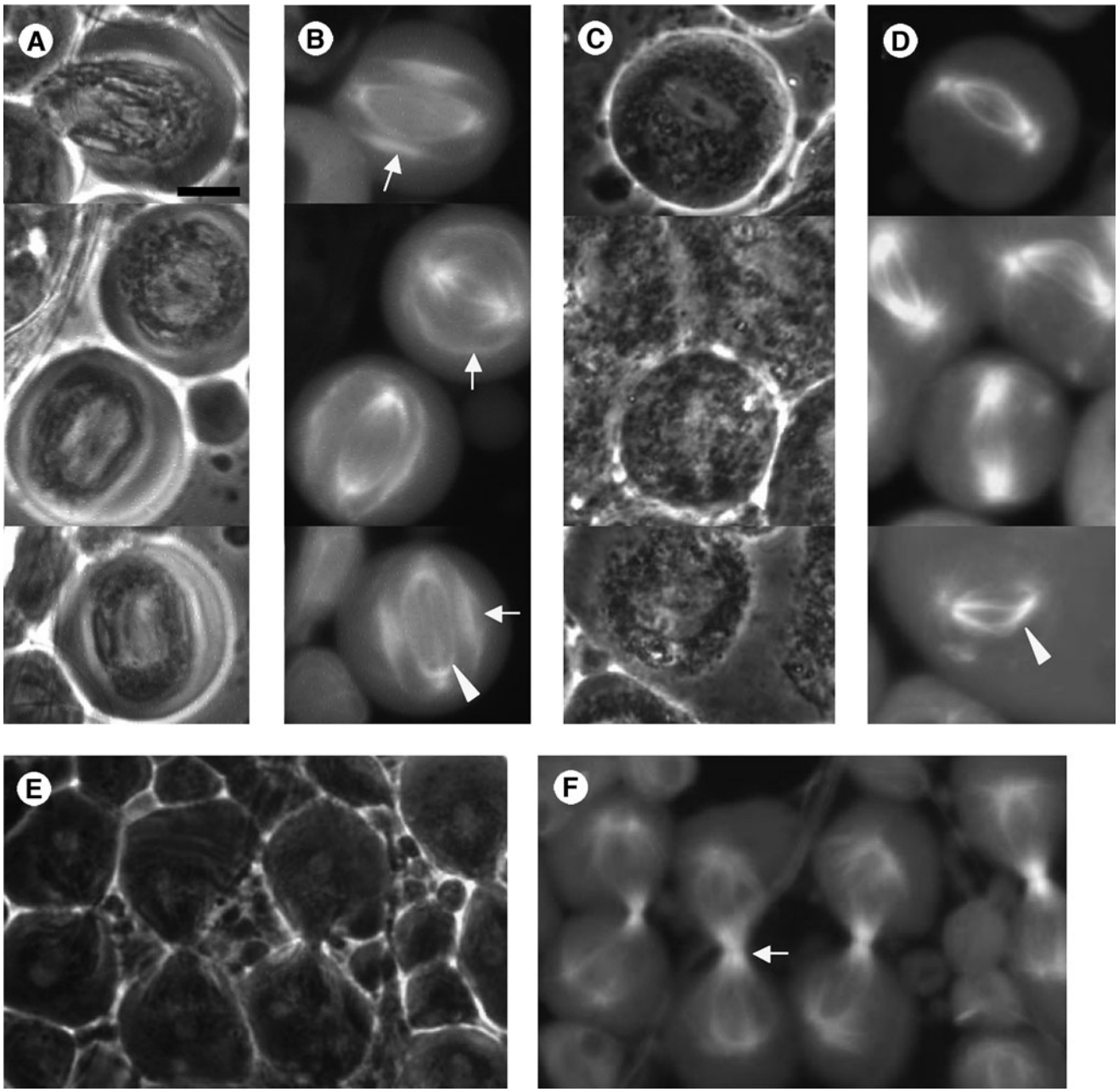

FIG. 4. Meiotic spindles do not form properly in *mtsh*. Phase-contrast (**A, C, E**) and fluorescence (**B, D, F**) micrographs of male meiotic cells from wild-type (**A, B, E, F**) and $mtsh^{Z2\text{-}2620}/mtsh^{Z2\text{-}2620}$ (**C, D**) flies carrying a β *tubulin-EGFP* transgene (gift from H. Oda and Y. Akiyama-Oda). Wild-type cells in meiosis I (**A, B**) have strongly fluorescent regions of overlapping microtubules from opposite asters (**B**, arrows), along with a region of the spindle (arrowhead) thought to be anastral and nucleated from the chromosomal region (Rebollo *et al.*, 2004). Cells from *mtsh* mutant males (**C, D**) do not have the overlapping astral spindle region and appear to contain only the anastral central spindle (**D**, arrowhead) plus some nonoverlapping astral microtubules. In wild-type cells at telophase I (**E, F**), strong fluorescence from the astral central spindle is detected in the region of the cleavage furrow and contractile ring (arrow). No such furrowing cells are ever observed in *mtsh* flies. The identical phenotype is seen in $mtsh^{Z2\text{-}2620}/mtsh^{Z2\text{-}3484}$ and $mtsh^{Z2\text{-}2620}/mtsh^{55207\text{-}12}$ transheterozygotes. Scale bar 10 μm.

Franklin-Dumont *et al.*, 2007). The *mtsh* mutant is the first identified in which both meiosis and spermiogenesis proceed though with lack of proper coordination.

All *mtsh* orthologs are predicted to encode a single polypeptide that matches the longer 649 amino acid predicted isoform of *D. melanogaster* Mtsh. Evolutionary conservation of the bromodomain-related region (which is predicted to be truncated in the shorter predicted *D. melanogaster* isoform) is consistent with functional relevance of the longer isoform. The prediction of the shorter isoform, which would result from inclusion of an additional 27-bp exon containing a stop codon, may be spurious, but it may alternatively reflect

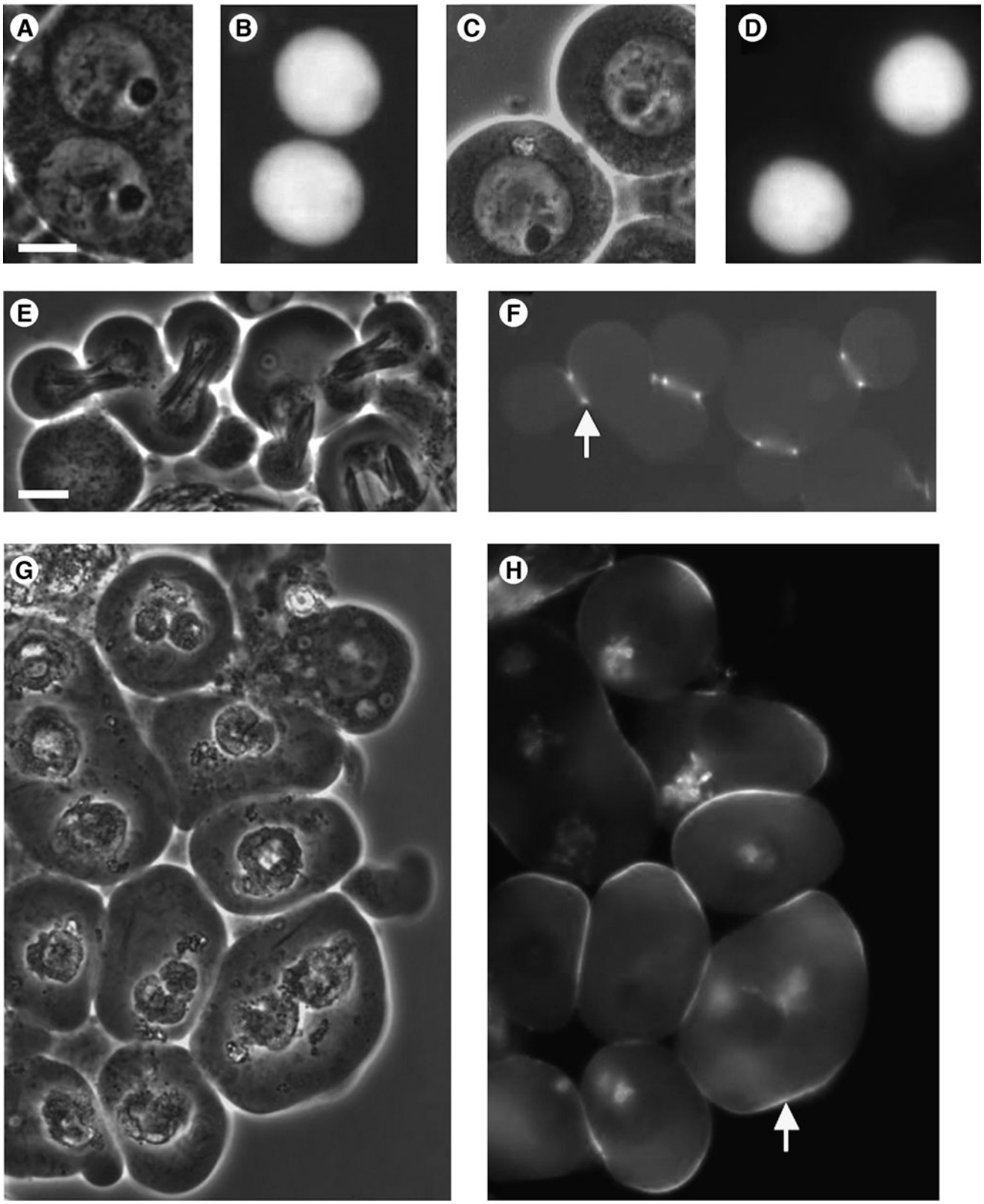

FIG. 5. Anillin is not properly localized to a contractile ring in *mtsh* meiotic cells. Phase-contrast (**A, C, E, G**) and fluorescence (**B, D, F, H**) micrographs of cells from wild-type (**A, B, E, F**) and $mtsh^{Z2\text{-}2620}/mtsh^{Z2\text{-}2620}$ (**C, D, G, H**) flies carrying a transgene encoding GFP-Anillin (Goldbach *et al.*, 2010). GFP-anillin is nuclear in wild-type (**A, B**) and *mtsh* (**C, D**) primary spermatocytes. In wild-type meiotic cells (**E, F**), GFP-anillin localizes to the contractile ring (arrow). In *mtsh* meiotic cells (**G, H**), no GFP-anillin-containing contractile rings are seen, though GFP-anillin has redistributed from the nucleus diffusely to the cell cortex (arrow). The identical phenotype is seen in $mtsh^{Z2\text{-}2620}/mtsh^{Z2\text{-}3484}$ and $mtsh^{Z2\text{-}2620}/mtsh^{55207\text{-}12}$ transheterozygotes. Scale bars 10 μm in (**A–D**), (**E–H**).

divergence of the *Drosophila* ortholog to a situation of regulation by alternative splicing. Indeed, a *D. melanogaster* testis EST matches the transcript encoding the isoform with the full bromodomain-related region, while an embryo EST matches the transcript encoding the truncated isoform.

The *mtsh* gene is detectably conserved only in Diptera, Coleoptera, and Lepidoptera. Mtsh and its orthologs have diverged fairly quickly overall in these insect lineages, perhaps reflecting mechanisms of reproductive isolation, as is common with genes involved in gametogenesis (Dorus *et al.*, 2006). Two regions of the protein are highly conserved, region 1 (highly alpha helical though with no recognizable motifs) in the amino terminal half of the protein, and region 2 near the carboxy terminus, which resembles a bromodomain both in sequence and in predicted alpha helical profile (Fig. 3B–E). Mtsh orthologs all show strikingly similar predicted alpha helical profiles in this region.

Bromodomains bind to acetylated lysine residues, typically on histones, and are found in some transcriptional regulators, histone acetyltransferases, and other chromatin remodeling factors (reviewed in Loyola and Almouzni, 2004). These domains are typically around 110 amino acids and encompass four alpha helices, α_Z, α_A, α_B, and α_C, with the loop between helices Z and A interacting with the loop between helices B and C. Some bromodomains contain a small fifth helix within the ZA loop. Ligands bind in a hydrophobic zone within the ZA–BC loop interaction. Region 2 in Mtsh is reminiscent of a bromodomain in size, alpha helical structure, and sequence, though only a subset of the highly conserved residues seen in bromodomains are retained (Fig. 3E). Notably, the three residues important for acetylated histone binding (arrows in Fig. 3D, E) (Mujtaba *et al.*, 2007), including the BC loop asparagine that forms a crucial hydrogen bond with the acetyl-lysine carbonyl group (reviewed in Zeng and Zhou, 2002), are not conserved in Mtsh. Mtsh orthologs instead include an invariant leucine at the position corresponding to the BC loop asparagine, suggesting the possibility of different ligand sensitivity.

The nonconservation of acetyl-lysine binding residues is consistent with the possibility that Mtsh may serve a role other than chromatin binding. Alternatively, Mtsh may, like other bromodomain family proteins, participate in chromatin binding and transcriptional regulation but with different ligand selectivity. A possible role for Mtsh as a chromatin-binding protein would be consistent with its coordination of meiosis and spermiogenesis in spermatogenesis, as many of the known genes involved in that process function in transcriptional activation; Mtsh may activate transcription of meiotic cell cycle regulators, such that meiotic progression is delayed in *mtsh* flies, or it may control expression of translational repressors of spermiogenesis genes, such that spermiogenesis is activated early in *mtsh* testes. Mtsh may instead be part of the yet-uncharacterized link between the *can*-class TAFs and translational activation of the testis *cdc25* homolog *twine.* Assessment of *mtsh* expression in *can*-class mutants and Twine in *mtsh* mutants will in the future test this hypothesis. Exploration of these possibilities will elucidate whether the *mtsh* phenotype can be defined precisely as premature spermiogenesis, delayed meiosis, or both.

Meiotic cytokinesis does not occur in *mtsh* mutant males. Microtubule observation in *mtsh* testes showed a meiosis I spindle defect in a region of overlapping antipolar microtubules. Such a region of interdigitating microtubules is often called the central spindle, but that term is imprecise in that it does not differentiate whether the microtubules originate from the asters or from the distinct anastral portion of the spindle nucleated in the chromosomal region (Rebollo *et al.*, 2004). The *mtsh* mutant appears to lack interdigitating astral microtubules in male meiotic cells, while the anastral spindle appears intact. It is well established that in many cell types, positional signals from the central spindle to the cell cortex determine the location of the contractile ring. Conflicting reports on *Drosophila* male meiosis indicate, alternately, that the central region of the astral spindle (Rebollo *et al.*, 2004) or the anastral spindle (Bonaccorsi *et al.*, 1998) is essential for determining contractile ring placement. Our results support the hypothesis that the aster-derived central spindle helps position the contractile ring, since in *mtsh* only the anastral central spindle forms, but the contractile ring components anillin and Sep2 are not properly localized.

We speculate that the failure of meiotic cytokinesis in *mtsh* homozygous males, via aberrant spindle and contractile ring construction, is ultimately a secondary effect of faulty developmental coordination. Previous work from other researchers suggests a role for mitochondria in establishing or stabilizing the meiotic central spindle. The Infertile crescent (Ifc) protein, a sphingolipid desaturase (Ternes *et al.*, 2002), is associated both with mitochondria during meiosis as well as later with the meiotic contractile ring (Basu and Li, 1998). In the absence of Ifc, central spindles are not properly assembled or stabilized, and meiotic cytokinesis fails (Basu and Li, 1998). Mitochondria are thought to travel on microtubule tracks in *Drosophila* spermatogenesis (reviewed in Hales, 2004; Aldridge *et al.*, 2007). In wild type, mitochondria associate in the midzone of the meiotic spindle, presumably in association with plus-end-directed microtubule motors; later, in early round spermatids, mitochondria aggregate toward the minus ends of microtubules (reviewed in Fuller, 1993). If the signal for mitochondrial aggregation occurs prematurely, before spindle formation, the shell-like fused mitochondrial structure surrounding *mtsh* spermatocyte nuclei may reflect the premeiotic pattern of microtubules. Improper mitochondrial localization in *mtsh* mutant cells may therefore prevent Ifc from helping to stabilize the astral central spindle and establish the equatorial plane where the contractile ring would otherwise form. (The causal relationship could instead be reversed, though this is less likely given the chronology of events and the normal centrosome migration in *mtsh*.) Another possibility is that the mitochondrial shell prevents the transfer of chromosomal passenger proteins to the cell cortex, where they would normally trigger early events of cytokinesis (Ruchaud *et al.*, 2007). Consistent with either hypothesis, GFP-anillin and Sep2-GFP fail to localize properly in *mtsh* meiotic cells. Our observation of some anillin cortical localization fits with previous observations that anillin associates diffusely with the cell cortex in the absence of central spindle-related signals like Pebble (reviewed in Hickson and O'Farrell, 2008).

Conclusions

Proper coordination of meiosis and spermiogenesis in *D. melanogaster* spermatogenesis requires the function of a novel gene, *mtsh*, which encodes a protein with a predicted

bromodomain-related region. Mtsh is conserved in some insect lineages. In the absence of functional Mtsh, events of sperm tail growth such as mitochondrial aggregation and fusion precede and accompany meiotic onset. Meiotic nuclear division subsequently occurs; however, meiotic cytokinesis fails in *mtsh* as a result of faulty central spindle and contractile ring formation, both likely secondary effects of aberrant mitochondrial localization.

Acknowledgments

The authors thank the 119 undergraduate genetics students at Davidson College from the Fall 2002, 2003, 2004, and 2007 semesters for their participation in deficiency mapping and P element excision screens. The authors are grateful to Julie Brill, Phil Goldbach, and other members of the Brill Lab for hospitality, fly stocks, and comments on the project. The authors thank H. Oda, Y. Akiyama-Oda, C. Zuker, B. Wakimoto, D. Lindsley, and the Bloomington and Szeged Drosophila Stock Centers for fly stocks. The FlyBase and FlyAtlas databases provided crucial information. Members of the Biology Department at Davidson College, including M. Campbell, S. Sarafova, K. Bernd, D. Wessner, B. Lom, and C. Healey, contributed help with equipment and general advice. Work in the Hales lab has been supported by National Science Foundation CAREER Grant 0133335, National Institutes of Health AREA Grant R15GM080689, and Davidson College.

Disclosure Statement

No competing financial interests exist.

References

Aldridge, A.C., Benson, L.P., Siegenthaler, M.M., Whigham, B.T., Stowers, R.S., and Hales, K.G. (2007). Roles for Drp1, a dynamin-related protein, and milton, a kinesin-associated protein, in mitochondrial segregation, unfurling and elongation during *Drosophila* spermatogenesis. Fly (Austin) **1,** 38–46.

Alphey, L., Jimenez, J., White-Cooper, H., Dawson, I., Nurse, P., and Glover, D.M. (1992). Twine, a cdc25 homolog that functions in the male and female germline of *Drosophila*. Cell **69,** 977–988.

Altschul, S.F., Gish, W., Miller, W., Myers, E.W., and Lipman, D.J. (1990). Basic local alignment search tool. J Mol Biol **215,** 403–410.

Baker, C.C., and Fuller, M.T. (2007). Translational control of meiotic cell cycle progression and spermatid differentiation in male germ cells by a novel eIF4G homolog. Development **134,** 2863–2869.

Barr, F.A., and Gruneberg, U. (2007). Cytokinesis: placing and making the final cut. Cell **131,** 847–860.

Basu, J., and Li, Z. (1998). The Des-1 protein, required for central spindle assembly and cytokinesis, is associated with mitochondria along the meiotic spindle apparatus and with the contractile ring during male meiosis in *Drosophila melanogaster*. Mol Gen Genet **259,** 664–673.

Bonaccorsi, S., Giansanti, M.G., and Gatti, M. (1998). Spindle self-organization and cytokinesis during male meiosis in asterless mutants of *Drosophila melanogaster*. J Cell Biol **142,** 751–761.

Brill, J.A., Hime, G.R., Scharer-Schuksz, M., and Fuller, M.T. (2000). A phospholipid kinase regulates actin organization and intercellular bridge formation during germline cytokinesis. Development **127,** 3855–3864.

Chintapalli, V.R., Wang, J., and Dow, J.A. (2007). Using FlyAtlas to identify better *Drosophila melanogaster* models of human disease. Nat Genet **39,** 715–720.

Cokol, M., Nair, R., and Rost, B. (2000). Finding nuclear localization signals. EMBO Rep **1,** 411–415.

Courtot, C., Fankhauser, C., Simanis, V., and Lehner, C.F. (1992). The *Drosophila* cdc25 homolog twine is required for meiosis. Development **116,** 405–416.

Dhalluin, C., Carlson, J.E., Zeng, L., He, C., Aggarwal, A.K., and Zhou, M.M. (1999). Structure and ligand of a histone acetyltransferase bromodomain. Nature **399,** 491–496.

Dorus, S., Busby, S.A., Gerike, U., Shabanowitz, J., Hunt, D.F., and Karr, T.L. (2006). Genomic and functional evolution of the *Drosophila melanogaster* sperm proteome. Nat Genet **38,** 1440–1445.

Franklin-Dumont, T.M., Chatterjee, C., Wasserman, S.A., and Dinardo, S. (2007). A novel eIF4G homolog, off-schedule, couples translational control to meiosis and differentiation in *Drosophila* spermatocytes. Development **134,** 2851–2861.

Fuller, M.T. (1993). Spermatogenesis. In *The Development of* Drosophila melanogaster. M. Bate and A. Martinez-Arias, eds. (Cold Spring Harbor Press, Cold Spring Harbor, NY), pp. 71–147.

Gao, D., and McHenry, C.S. (2001). Tau binds and organizes *Escherichia coli* replication proteins through distinct domains. Domain III, shared by gamma and tau, binds delta delta′ and chi psi. J Biol Chem **276,** 4447–4453.

Glover, B.P., Pritchard, A.E., and McHenry, C.S. (2001). Tau binds and organizes *Escherichia coli* replication proteins through distinct domains: domain III, shared by gamma and tau, oligomerizes DnaX. J Biol Chem **276,** 35842–35846.

Goldbach, P., Wong, R., Sarpal, R., and Brill, J.A. (2010). Stabilization of the actomyosin ring enables spermatocyte cytokinesis in *Drosophila*. Mol Biol Cell (In press).

Hales, K.G. (2004). The machinery of mitochondrial fusion, division, and distribution, and emerging connections to apoptosis. Mitochondrion **4,** 285–308.

Hales, K.G., and Fuller, M.T. (1997). Developmentally regulated mitochondrial fusion mediated by a conserved, novel, predicted GTPase. Cell **90,** 121–129.

Hickson, G.R., and O'Farrell, P.H. (2008). Anillin: a pivotal organizer of the cytokinetic machinery. Biochem Soc Trans **36,** 439–441.

Hiller, M., Chen, X., Pringle, M.J., Suchorolski, M., Sancak, Y., Viswanathan, S., Bolival, B., Lin, T.Y., Marino, S., and Fuller, M.T. (2004). Testis-specific TAF homologs collaborate to control a tissue-specific transcription program. Development **131,** 5297–5308.

Horton, P., Park, K.J., Obayashi, T., Fujita, N., Harada, H., Adams-Collier, C.J., and Nakai, K. (2007). WoLF PSORT: protein localization predictor. Nucleic Acids Res **35,** W585–W587.

Jarvis, T.C., Beaudry, A.A., Bullard, J.M., Janjic, N., and McHenry, C.S. (2005). Reconstitution of a minimal DNA replicase from *Pseudomonas aeruginosa* and stimulation by non-cognate auxiliary factors. J Biol Chem **280,** 7890–7900.

Koundakjian, E.J., Cowan, D.M., Hardy, R.W., and Becker, A.H. (2004). The Zuker collection: a resource for the analysis of autosomal gene function in *Drosophila melanogaster*. Genetics **167,** 203–206.

Larkin, M.A., Blackshields, G., Brown, N.P., Chenna, R., McGettigan, P.A., McWilliam, H., Valentin, F., Wallace, I.M., Wilm, A., Lopez, R., Thompson, J.D., Gibson, T.J., and Higgins, D.G. (2007). Clustal W and Clustal X version 2.0. Bioinformatics **23,** 2947–2948.

Loyola, A., and Almouzni, G. (2004). Bromodomains in living cells participate in deciphering the histone code. Trends Cell Biol **14,** 279–281.

Maines, J.Z., and Wasserman, S.A. (1999). Post-transcriptional regulation of the meiotic Cdc25 protein Twine by the Dazl orthologue Boule. Nat Cell Biol **1,** 171–174.

Marchler-Bauer, A., Anderson, J.B., Chitsaz, F., Derbyshire, M.K., DeWeese-Scott, C., Fong, J.H., Geer, L.Y., Geer, R.C., Gonzales, N.R., Gwadz, M., He, S., Hurwitz, D.I., Jackson, J.D., Ke, Z., Lanczycki, C.J., Liebert, C.A., Liu, C., Lu, F., Lu, S., Marchler, G.H., Mullokandov, M., Song, J.S., Tasneem, A., Thanki, N., Yamashita, R.A., Zhang, D., Zhang, N., and Bryant, S.H. (2009). CDD: specific functional annotation with the Conserved Domain Database. Nucleic Acids Res **37,** D205–D210.

McHenry, C.S. (2003). Chromosomal replicases as asymmetric dimers: studies of subunit arrangement and functional consequences. Mol Microbiol **49,** 1157–1165.

Mikhaylova, L.M., Boutanaev, A.M., and Nurminsky, D.I. (2006). Transcriptional regulation by Modulo integrates meiosis and spermatid differentiation in male germ line. Proc Natl Acad Sci U S A **103,** 11975–11980.

Mujtaba, S., Zeng, L., and Zhou, M.M. (2007). Structure and acetyl-lysine recognition of the bromodomain. Oncogene **26,** 5521–5527.

Nair, R., and Rost, B. (2005). Mimicking cellular sorting improves prediction of subcellular localization. J Mol Biol **348,** 85–100.

Rebollo, E., Llamazares, S., Reina, J., and Gonzalez, C. (2004). Contribution of noncentrosomal microtubules to spindle assembly in *Drosophila* spermatocytes. PLoS Biol **2,** E8.

Rost, B., and Sander, C. (1993). Prediction of protein secondary structure at better than 70% accuracy. J Mol Biol **232,** 584–599.

Rost, B., Yachdav, G., and Liu, J. (2004). The PredictProtein server. Nucleic Acids Res **32,** W321–W326.

Ruchaud, S., Carmena, M., and Earnshaw, W.C. (2007). Chromosomal passengers: conducting cell division. Nat Rev Mol Cell Biol **8,** 798–812.

Ryder, E., Blows, F., Ashburner, M., Bautista-Llacer, R., Coulson, D., Drummond, J., Webster, J., Gubb, D., Gunton, N., Johnson, G., O'Kane, C.J., Huen, D., Sharma, P., Asztalos, Z., Baisch, H., Schulze, J., Kube, M., Kittlaus, K., Reuter, G., Maroy, P., Szidonya, J., Rasmuson-Lestander, A., Ekstrom, K., Dickson, B., Hugentobler, C., Stocker, H., Hafen, E., Lepesant, J.A., Pflugfelder, G., Heisenberg, M., Mechler, B., Serras, F., Corominas, M., Schneuwly, S., Preat, T., Roote, J., and Russell, S. (2004). The DrosDel collection: a set of P-element insertions for generating custom chromosomal aberrations in *Drosophila melanogaster*. Genetics **167,** 797–813.

Sigrist, S., Ried, G., and Lehner, C.F. (1995). Dmcdc2 kinase is required for both meiotic divisions during *Drosophila* spermatogenesis and is activated by the Twine/cdc25 phosphatase. Mech Dev **53,** 247–260.

Silverman-Gavrila, R.V., Hales, K.G., and Wilde, A. (2008). Anillin-mediated targeting of peanut to pseudocleavage furrows is regulated by the GTPase Ran. Mol Biol Cell **19,** 3735–3744.

Ternes, P., Franke, S., Zahringer, U., Sperling, P., and Heinz, E. (2002). Identification and characterization of a sphingolipid delta 4-desaturase family. J Biol Chem **277,** 25512–25518.

Tweedie, S., Ashburner, M., Falls, K., Leyland, P., McQuilton, P., Marygold, S., Millburn, G., Osumi-Sutherland, D., Schroeder, A., Seal, R., and Zhang, H. (2009). FlyBase: enhancing *Drosophila* Gene Ontology annotations. Nucleic Acids Res **37,** D555–D559.

Voelker, R.A., Greenleaf, A.L., Gyurkovics, H., Wisely, G.B., Huang, S.M., and Searles, L.L. (1984). Frequent imprecise excision among reversions of a P element-caused lethal mutation in *Drosophila*. Genetics **107,** 279–294.

Wakimoto, B.T., Lindsley, D.L., and Herrera, C. (2004). Toward a comprehensive genetic analysis of male fertility in *Drosophila melanogaster*. Genetics **167,** 207–216.

White-Cooper, H. (2010). Molecular mechanisms of gene regulation during *Drosophila* spermatogenesis. Reproduction **139,** 11–21.

White-Cooper, H., Alphey, L., and Glover, D.M. (1993). The cdc25 homologue twine is required for only some aspects of the entry into meiosis in *Drosophila*. J Cell Sci **106,** 1035–1044.

Zeng, L., and Zhou, M.M. (2002). Bromodomain: an acetyl-lysine binding domain. FEBS Lett **513,** 124–128.

Address correspondence to:
Karen G. Hales, Ph.D.
Department of Biology
Davidson College
Box 7118
Davidson, NC 28035

E-mail: kahales@davidson.edu

Received for publication November 1, 2009; received in revised form March 29, 2010; accepted March 30, 2010.